A NaI(Tl)-based radioactive noble-gas monitoring system used for radiation monitoring

HuiBin Li [*], WeiGuo Lei, TianCheng Feng, DingWei Huang, ZiNing Tian

Northwest Institute for Nuclear Technology, P.O. Box 69-27, Xi'an, 710024, Shanxi, China

ARTICLE INFO

ABSTRACT

Radioactive noble-gas monitoring is necessary in nuclear facilities. A NaI(Tl)-based radioactive noble-gas monitoring system was developed. In order to increase the amount of air to be measured, the sample vessel of this system was larger than that of other systems, and was pressurized to about 5×10^5 Pa. In a laboratory experiment, technical ways to reduce the memory effect were investigated. In field tests, a method of spectra analysis was established and calibration coefficients and minimum detectable concentrations of ^{133}Xe, ^{135}Xe and ^{41}Ar were calculated. Finally, detection ability was compared with other online monitoring systems.

1. Introduction

Radiation safety is a crucial issue during the lifetime of nuclear reactors and other nuclear facilities. In order to protect people and the environment from ionizing radiation, various monitoring equipment should be installed surrounding the nuclear facility. The monitoring objects should at least include environmental gamma-ray dose rate, radioactive aerosols, radioactive iodine, and radioactive noble gases. If a leakage accident occurs, radioactive noble gases are more easily spread through cracks and released to the environment than solid fission nuclides which turn into radioactive aerosols later. Thus, monitoring of radioactive noble gases is more sensitive than other techniques.

There are various categories of equipment that can be used to monitor radioactive noble gases. The NGM 204 is a commonly used (Mirion, 2002), in which a dual silicon diode detector is integrated in a 300-mL sample volume surrounded by a 5-cm lead shield. One silicon diode detector measures beta/gamma radiation from the sample vessel and environmental gamma radiation; and the other detects gamma radiation from the sample vessel and environmental gamma radiation. Then beta counts originating from the sample can be obtained by dynamic gamma compensation. Structure of this kind of equipment is simple, so it is cost effective and can be widely used. However, because the measured gas volume is limited and the background radiation is not sufficiently reduced, the minimum detectable concentration (MDC) is high, at about 10^4 Bq/m^3. Additionally, categories of radioactive gases cannot be distinguished.

Another type of radioactive noble-gas monitoring system is xenon sampling, purifying, and measurement equipment, such as ARSA (Cooper, 2007) and SAUNA (Ringbom, 2003), which extract about 1 mL of pure xenon from several cubic meters of air, then the xenon sample is measured by the beta–gamma coincidence technique. Because the sampling volume is large, and the background radiation is obviously reduced by the coincidence technique and the surrounding shield, the MDC is below 1 mBq/m^3 for four xenon radioactive isotopes. Structure of this equipment is complicated, and it is too expensive to be widely used. However, a very low MDC level is unnecessary for radiation protection monitoring purposes and such equipment is only suitable for Comprehensive Nuclear-Test-Ban Treaty verification.

This paper presents new equipment used for radioactive noble-gas monitoring. The noble gas is not purified in the equipment but is directly measured, structure of the equipment is as simple as for NGM 204 but the MDC is reduced by two orders of magnitude, and so it can be widely used.

2. Equipment design and manufacture

2.1. Equipment design

In order to distinguish categories of radioactive noble gases, gamma-rays emitted by the nuclides are measured. High-purity germanium (HPGe) systems were acceptable from a technical viewpoint but were ruled out due to high price and high maintenance requirements, so a 7.6 cm × 7.6 cm NaI(Tl) detector was used.

In order to reduce the MDC, three approaches can be applied:

---

increasing the volume of air to be measured, increasing detection efficiency, and reducing ambient background radiation. For monitoring systems that do not separate and purify xenon, the volume of air to be measured is equal to the capacity of the sample vessel, which should be as large as possible, and should be pressurized to several atmospheres to increase the amount of air to be measured. In order to increase the detection efficiency, the gamma-ray detector should be placed in the center of the sample vessel. Ambient background counts can be reduced by shielding or by the coincidence technique; however, the latter cannot be used in this system as the volume of the air to be measured is too small.

A schematic view of the equipment is shown in Fig. 1. An aerosol filter is placed in the monitoring location, and is connected to Valve 1 via a plastic tube. Ordinary online monitoring devices use 5-cm lead shield, but this system's lead shield is 10 cm. Increasing thickness of the lead shield can obviously reduce the background count rate and improve the detection ability, but weight and volume of the equipment increases also. In order to solve this problem, the lead shielding is not an integral part, but is assembled by several standard lead bricks. In addition, 2-mm thick cadmium and 1-mm thick copper layers are placed inside the lead shielding to shield the X-rays emitted by lead and cadmium. Capacity of the sample vessel is 5.2 L, and a well is opened in the center of it. The sample vessel is inserted into the radiation shielding, and the NaI(Tl) detector and the associated photomultiplier tube is inserted in the well in the center of the sample vessel. In order to reduce the attenuation effect, the sample vessel is manufactured of aluminum, and the thickness of the wall between the sample and the NaI(Tl) detector is only 3 mm. However, to ensure the sample vessel can endure high pressure without deformation, the thickness of the outer wall is 8 mm. A Digibase-E multichannel analyzer is used to process the signal, and is connected to a remote control computer via a network. All measured spectra are stored in the control computer for later re-analysis, together with various sensor information used for state-of-health monitoring.

2.2. Monitoring cycle setting

In each monitoring cycle, a background spectrum is measured before sampling and measurement. Then opening Valve 5 and the diaphragm vacuum pump, residual air in the sample vessel is evacuated in about 2 min. Pressure in the sample vessel is monitored by the pressure gauge. After that, Valve 1, Valve 6 and the compression pump are opened; the air in the monitoring location is injected in the pipeline before Valve 4, and returns to the same location via the return tube. Air flow rate is measured by the flow meter. In order to completely replace the remaining air in the pipeline with the air in the monitoring location before Valve 4, cumulative volume of the air passing through the flow meter should be at least three times the capacity of the plastic tube connecting the equipment and monitoring location. Then closing the compression pump and Valve 6, and opening Valves 3 and 4, air in the pipeline is injected into the sample vessel. The pressure is also monitored by the pressure gauge. When the pressure reaches about 10^5 Pa, Valve 3 is closed, and the compression pump runs again until the pressure reaches about 5×10^5 Pa. Finally, the air contained in the sample vessel is measured by the NaI(Tl) detector; measurement time can be set arbitrarily and the measured spectrum is displayed on the remote control computer. After the measurement, the air contained in the sample vessel is released to the return tube via Valves 4 and 6 at first, and is then evacuated by the diaphragm vacuum pump.

Total count rate of the measured sample spectrum is compared with that of the preceding background spectrum. If the increased count rate is lower than the preset value, e.g. 0.8, it can be concluded that there is no contamination in the air, and another sampling and measurement cycle is run. Otherwise, the cleaning process is run. The sample is removed by repeated pumping and flushing. The cleaning process consists of 5×2 min of pumping. In between each pumping, the sample vessel is filled with nitrogen released by opening Valve 2. After the cleaning process, the residual activity is again measured by the NaI(Tl) detector in order to obtain the new background spectrum used for subsequent calculation.

3. Methods used to reduce memory effect

An important drawback with the continuous radioactive noble-gas monitoring system is that part of the noble gas diffuses into the walls of the sample vessel during the measurement, even after it has been removed by the pump-and-flush cycle (Bläckberg, 2011, 2013; Yongchun, 2017). The residual activity left in the sample vessel is often known as the "memory effect". The memory effect elevates the MDC of the system, especially when the preceding sample exhibits high radioactivity. It has been reported that Al_2O_3, Al or SiO_2 coated on the surface of a plastic scintillator detector can effectively reduce the memory effect, and these materials can be used as a noble gas diffusion barrier (Bläckberg, 2011, 2013; Yongchun, 2017). Thus the sample vessel was made of aluminum, and its memory effect was tested with radioactive xenon.

3.1. Memory effect test scheme

A quartz glass ampoule was filled with 100 μg of U_3O_8 and then irradiated by thermal neutrons in a reactor. After waiting one day until radioactive krypton isotopes had completely disintegrated, the quartz was plugged into a brass tube installed in the apparatus used to inject radioactive gas. Cracking the glass ampoule released radioactive gas into the sample vessel. The charge time was recorded as the reference time. Then nitrogen gas was injected into the sample vessel until its pressure reached 5×10^5 Pa. Then xenon was allowed to diffuse into the sample vessel walls for 10,000 s. Then the radioactive xenon in the sample
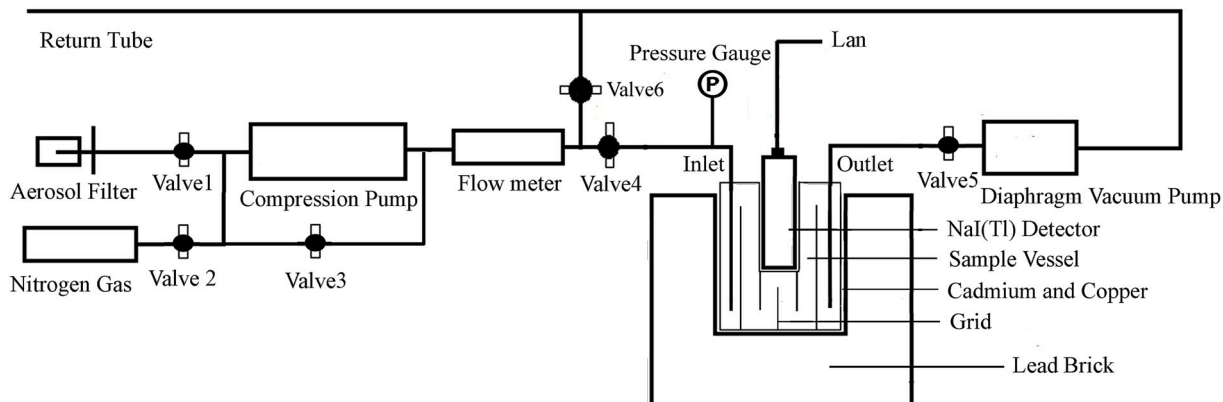

Fig. 1. Schematic view of the radioactive noble-gas monitoring equipment.

vessel was measured by the inserted NaI(Tl) spectrometer (Fig. 1). The measurement time was 1000 s and the acquired spectrum denoted as SP_0.

Then the cleaning process was run as described above, consisting of five pump-and-flush cycles. In between each cycle, the residual activity was measured by NaI(Tl) spectrometer. The measurement time was also 1000 s. A total of five spectra were acquired in the cleaning process, and denoted SP_1, SP_2…SP_5, respectively.

The residual percentage R_i is defined as the ratio of the amount of xenon still existing in the sample vessel after i times of pump-and-flush to the amount of xenon gas initially injected into the sample vessel, where i is 1–5. The measured peak counts in different spectra were corrected for decay and R_i was calculated using Eq. (1):

$$R_i = \frac{n_i \cdot e^{\lambda t_i} \cdot (1 - e^{-\lambda T_0})}{n_0 \cdot e^{\lambda t_0} \cdot (1 - e^{-\lambda T_i})} \times 100\% \qquad (1)$$

where n_i is 250-keV net peak count in SP_i, λ is the decay constant of ^{135}Xe, t_i is the time interval between the initial moment of acquiring SP_i and the reference time, T_i is the measurement time of SP_i, n_0 is 250-keV net peak count in SP_0, t_0 is the time interval between the initial moment of acquiring SP_0 and the reference time, and T_0 is the measurement time of SP_0.

3.2. Method used to reduce the memory effect

In the original design, no grid was set in the sample vessel. Its memory effect was tested eight times using ^{135}Xe. The measured residual percentages R_i for the sample vessel with no grid are listed in Table 1.

Two conclusions can be made according to Table 1. First, most of the sample is evacuated in the first pump-and-flush cycle, and increasing the number of pump-and-flush cycles does not effectively remove the adsorbed noble gas. Second, the residual percentage R_i is too high compared to previous reports (Bläckberg, 2011, 2013; Yongchun, 2017). There are two reasons for this: high pressure in the sample vessel makes the noble gas more easily diffuse into aluminum; and capacity of the sample is obviously larger than those used in other measurement systems.

Consequently, grids were installed in the sample vessel. The function of the grids is to separate the sample vessel into several small spaces, but those spaces are all connected (Fig. 1). Thus an internal tube is formed in the sample vessel. During the nitrogen gas flushing, nitrogen gas passes through the walls and the grids at high speed, and the noble gas adsorbed on the walls and the grids is more easily blown away. In order to reduce the attenuation effect of the grids, they were also made of aluminum of thickness of only 0.6 mm. The Monte Carlo simulations showed that the attenuation effect of the grids reduced detection efficiencies of 81-, 250-, and 1294-keV gamma-rays by 4, 2, and 1%, respectively.

The sample vessel with grids was also tested eight times using ^{135}Xe (Table 1). The initial and final measured spectra (SP_0 and SP_5, respectively) after five pump-and-flush cycles are shown in Fig. 2. The grids played an important role in reducing adsorption by about one order of magnitude (Table 1 and Fig. 2) and so were necessary in this large-capacity sample vessel.

Table 1
Residual percentages for sample vessel with and without grid after each pump-and-flush cycle.

1. Residual percentage	Without grid (%)	With grid (%)
R_1	28.1 ± 3.2	11.4 ± 2.7
R_2	14.6 ± 4.4	3.9 ± 0.62
R_3	13.9 ± 3.6	2.5 ± 0.52
R_4	13.7 ± 4.1	1.9 ± 0.43
R_5	13.4 ± 4.5	1.4 ± 0.45

4. Field test and calculation

4.1. Field test

The system was then tested in a nuclear power plant by measuring radioactive gases released by different systems. Radioactive gases released by main heat transfer system were ^{133}Xe and ^{135}Xe. The background spectrum was first measured followed by the sample spectrum. A typical group of spectra is shown in Fig. 3. Radioactive gases released by non-main heat transfer system were ^{133}Xe and ^{41}Ar. A typical result is shown in Fig. 4.

Characteristic peaks of ^{133}Xe and ^{135}Xe are shown in the sample spectrum (Fig. 3). The ^{133}Xe and ^{135}Xe emit 30.6- and 30.9-keV X-rays, so their peaks also appeared in the sample spectrum. In the background spectrum, a peak also appeared in the 81-keV region of interest (ROI), due to 74–87-keV X-rays emitted by the lead shielding and the residual ^{133}Xe left in the sample vessel after the cleaning process.

In Fig. 5, the 1294-keV peak from ^{41}Ar is clear and, similar to Fig. 3, peaks appeared in the 81-keV ROI in both the background and sample spectra, but the net count was much smaller.

4.2. Spectrum analysis

The purpose of the spectrum analysis process is to obtain the net counts generated by isotopes of interest in the sample. It is calculated using Eq. (2):

$$n_i = n_{si} - n_{bi} \qquad (2)$$

where, n_i is the net count generated by isotope of interest in the sample, n_{si} is the net count in the sample spectrum, and n_{bi} is the net count in the background spectrum for the same isotope. Three gaseous isotopes were measured in the experiment (^{133}Xe, ^{135}Xe and ^{41}Ar) and required separate calculations.

Net counts generated by ^{135}Xe and ^{41}Ar in the sample can be calculated using Eq. (2); however, whether Eq. (2) can be used for ^{133}Xe depends on measurement results. If the count generated by ^{133}Xe was obviously larger than that of the background radiation (Fig. 3), Eq. (2) could be used without inducing much error.

In Fig. 4, the count generated by ^{133}Xe in the 81-keV ROI is limited, but background counts caused by low energy gamma-rays and Compton scatter radiation generated by high energy gamma-ray in the same ROI are too high. Thus the sample's net count could not be accurately calculated by the method mentioned above. In this situation, the stripping method is a useful tool.

There are two steps in the spectrum stripping process: the background spectrum measured previously is subtracted from the measured spectrum after they are scaled to the same live time; and the ^{41}Ar standard spectrum is subtracted from the residual spectrum after the ^{41}Ar peak counts are scaled to the same number. Then the net count generated by ^{133}Xe in the sample can be easily identified and quantified in the stripped spectrum. The sample and stripped spectra are shown in Fig. 5.

It is clear that the background count rate in the 81-keV ROI is obviously reduced in Fig. 5, and the peak generated by ^{133}Xe can be clearly identified.

The ^{41}Ar standard spectrum was calculated based on the spectra measured in different situations, by combining two background-subtracted spectra with high and low ^{133}Xe/^{41}Ar ratios. They were combined in different proportions, until there was no contribution above the 81-keV ROI of ^{133}Xe.

The stripping method can also be used to deduct standard spectra of other isotopes, such as ^{135}Xe. However, it is useful only in situations in which Compton scatter radiation generated by ^{135}Xe or ^{135}Xe obviously increases the background count in the 81-keV ROI.

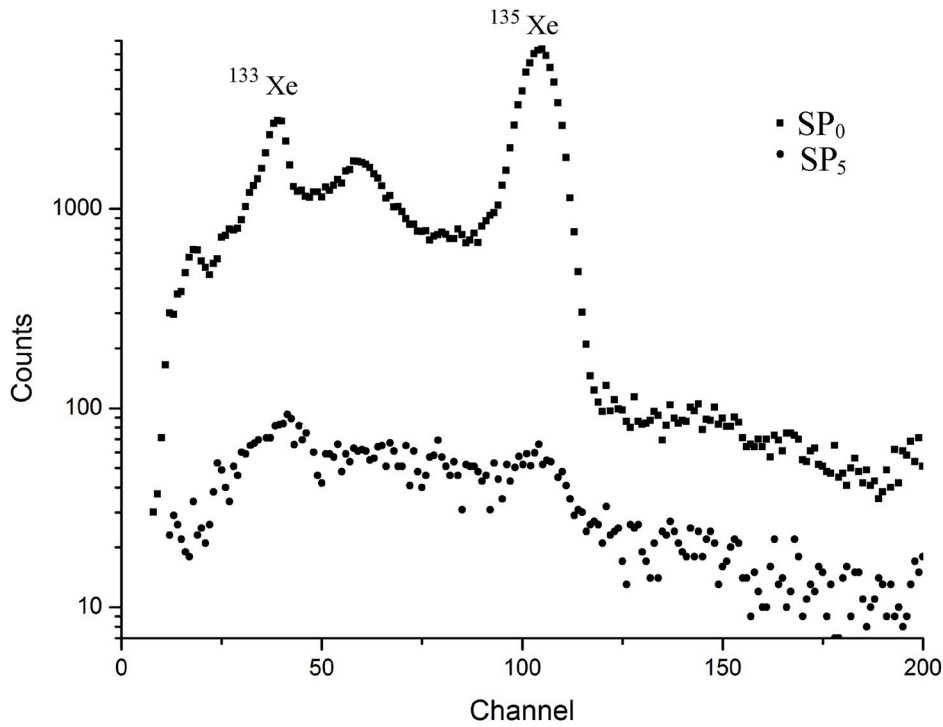As shown in Eq. (2), uncertainty of n_i is a combination of

Fig. 2. Initial spectrum and final measured spectrum after the cleaning process.
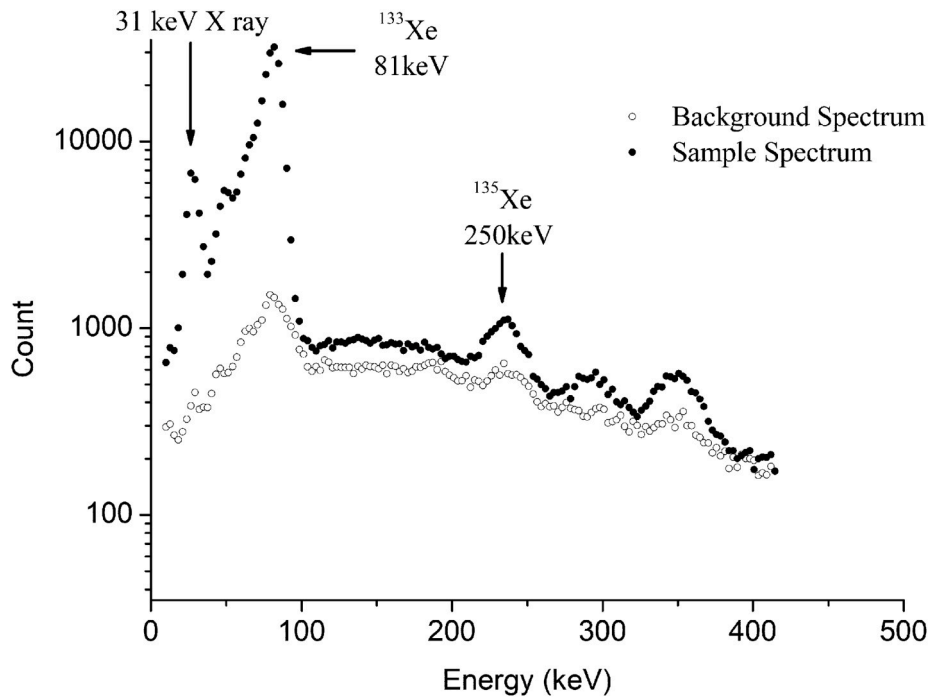

Fig. 3. Background and sample spectra measured in main heat transfer system.

uncertainties of n_{si} and n_{bi}, which can be read directly in the spectrum analysis software. Relative uncertainty of n_i is calculated using Eq. (3):

$$\frac{\sigma(n_i)}{n_i} = \frac{\sqrt{n_{si} + n_{bi}}}{n_{si} - n_{bi}} \times 100\% \tag{3}$$

If the stripping method is used, uncertainty induced by the stripping process must be added. This is mainly due to uncertainty of the stripped counts in the 81-keV ROI. This is a combination of uncertainties induced in the standard spectrum calculation and the peak-count scale factor of the measured and standard spectra.

If gaseous radioactive iodine also exists in the air, this system can measure it simultaneously. This will not seriously interfere with the measurement accuracy of ^{133}Xe and ^{135}Xe if the activity concentration of iodine is not too high.

4.3. System calibration

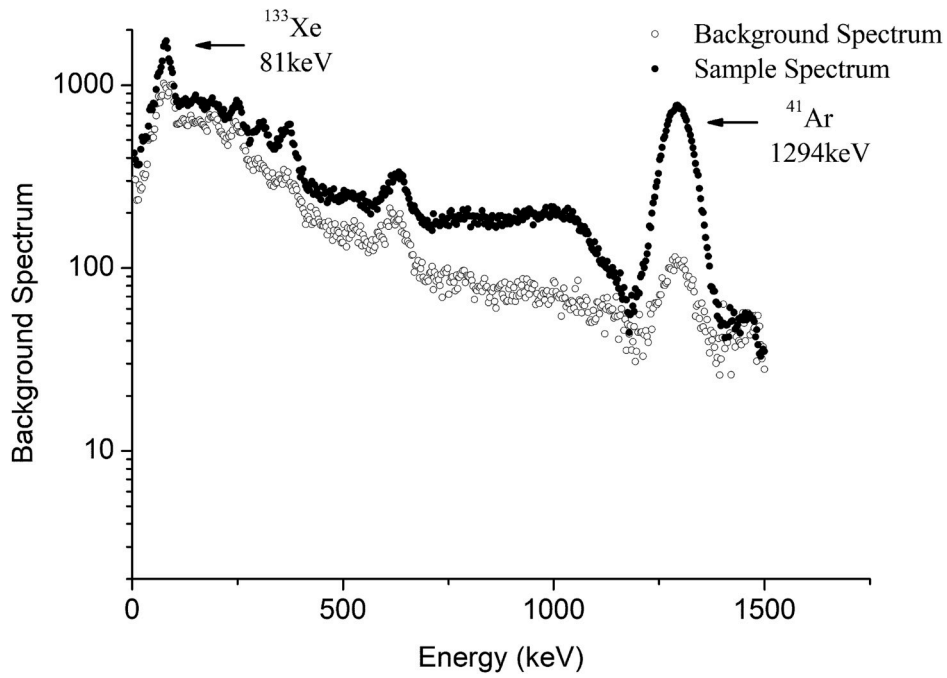The system was calibrated by comparing its results with that of the

Fig. 4. Background and sample spectra measured in non-main heat transfer system.
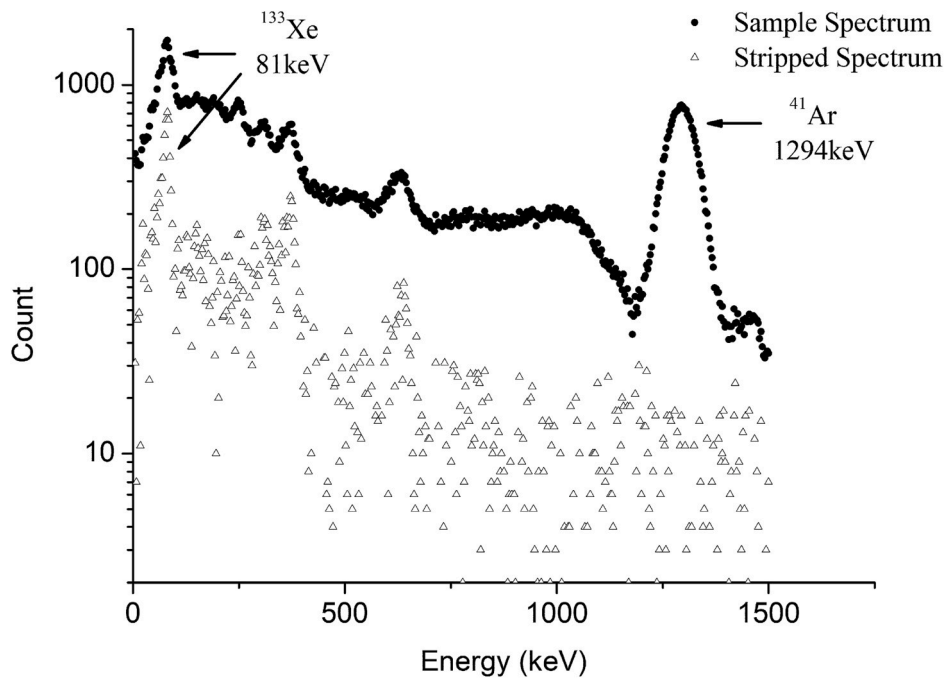

Fig. 5. Sample and stripped spectra measured in non-main heat transfer system.

laboratory HPGe gamma spectrometer. A temporary sampling tube and a stainless steel gas container were inserted between Valve 1 and the compression pump during the calibration process (Fig. 1). Capacity of the gas container was 1 L. In order to deduce attenuation effect of the gamma-rays, its window was made by carbon. One liter of air entered the gas container during the sampling process. Then it was measured by laboratory HPGe gamma spectrometer, so activity concentrations of various isotopes at the beginning of the sampling could be acquired. Based on the acquired net counts generated by the sample n_i, capacity of the sample vessel, measurement time, and interval between the beginning of the sampling and the beginning of the measurement, and

detection efficiencies of the above three isotopes can be obtained. In order to reduce uncertainties, each efficiency was calibrated at least five times, and then averages and standard deviations of the calibration results were calculated.

Uncertainty of detection efficiency is a combination of uncertainty of the laboratory HPGe gamma spectrometer measurement results and the standard deviations measured, and can be calculated using the error propagation equation. The calibration results are listed in Table 2.

The air concentration of the radioactive noble-gas (C_i) is calculated as follows:

Table 2
Detection efficiencies of characteristic gamma-rays emitted by three isotopes.

2. Isotope	Characteristic gamma-ray energy (keV)	Emission probability (%)	Detection efficiency (%)	Relative uncertainty (%)
^{133}Xe	81	36.5	6.22	8.2
^{135}Xe	250	90.0	4.06	6.5
^{41}Ar	1294	99.2	1.22	4.8

$$C_i = \frac{n_i \lambda_i}{\exp(-\lambda_i T_1)[1 - \exp(-\lambda_i T_2)]\varepsilon_i P_{\gamma i} V} \qquad (4)$$

where n_i is the net count generated by isotope of interest in the sample, calculated using Eq. (1); λ_i is the decay constant of the isotope; ε_i is the detection efficiency of gamma-rays; $P_{\gamma i}$ is emission probability of the measured gamma-rays; V is the volume of air at 1-atm of pressure, i.e. about 26 L; T_1 is the interval between the beginning of measurement and the beginning of sampling; and T_2 is the measurement time.

The uncertainties in the activity concentration are caused by the uncertainties of n_i and ε_i. The uncertainty of n_i is calculated using Eq. (2) and the uncertainty of ε_i is listed in Table 2. Final activity concentration uncertainty can be calculated by the error propagation equation. Error induced by other parameters in Eq. (4) can be ignored.

4.4. MDC calculation

An important system parameter is the MDC that can be achieved for a measurement. It can be estimated (at a confidence level of 95%) using Eq. (5):

$$MDC_i = \frac{3.3\sqrt{2n_b}\lambda_i}{\exp(-\lambda_i T_1)[1 - \exp(-\lambda_i T_2)]\varepsilon_i P_{\gamma i} V} \qquad (5)$$

where n_b is the total count in a certain ROI in the background spectrum. If no radioactive isotopes are detected in the subsequent sample measurement, the total count in the same ROI is equal to n_b.

In our laboratory and field testing, the background count rate of the spectrometer was measured. In ordinary radiation environment the integral background count rate for 0–3 MeV is about 7 cps. Because the shielding structure is similar to that of the laboratory gamma-ray spectrometer, the shielding effect is also similar.

The MDC values were calculated according to a sample spectrum with no artificial isotopes appearing and a background spectrum measured previously. The measurement time was 10,000 s for both. Because there was no artificial isotope in the sample vessel during the measurement process, the sample and background spectra were similar. The count rate of both spectra was 7.4. There are three steps to calculate the MDC: count rates in each ROI in the sample and background spectra are calculated; then $\sigma(n_i)$ is calculated using Eq. (2); and MDCs are obtained using Eq. (5). The background count rate in each ROI and the calculated MDCs are listed in Table 3.

The MDCs for three isotopes were in the range of 50–100 Bq/m^3, obviously below the MDC level of equipment such as NGM 204 (Table 3). The MDCs will rise if monitoring cycle is shortened. How long the monitoring cycle should be set depends on activity concentration of the air.

Setting grids in the sample vessel effectively reduced the memory effect, and so did the MDC level, although the detection efficiencies were reduced by setting them. Reduction of the MDC depends on the environmental radiation level and the activity concentration of the sample. The results in Fig. 2 are used as an example. The residual percentage was 1.4% after running the cleaning process, and the total count rate in the 250-keV ROI was 1.3 cps. If measurement time of the background and the subsequent sample spectra were both 10,000 s, then MDC was 57 Bq/m^3 in this background level. If no grids are set in the sample vessel, the residual percentage was 13.4%, so the total count in the 250-keV ROI

Table 3
The background count rate in each ROI and the MDCs for three isotopes.

3. Isotope	ROI range (keV)	Background count rate (cps)	MDC (Bq/m^3)
^{133}Xe	36–110	1.6	100
^{135}Xe	186–296	1.1	51
^{41}Ar	1220–1360	0.12	51

The background count rate and MDCs were calculated based on spectra measured in the ordinary environment, with no artificial isotopes appearing, and measurement time was 10,000 s.

is 3.5 cps, and the MDC will rise to 89 Bq/m^3 if the measurement time is the same.

5. Summary and conclusion

A system for automatic sampling and measurement of radioactive noble gas was developed. In order to increase the volume of air to be measured, the capacity of the sample vessel was increased to 5.2 L, and this was pressurized to 5×10^5 Pa by a compression pump.

The monitoring cycle of the equipment was designed. The background spectrum was measured at first, then the sample vessel was evacuated and the air in the monitoring location injected into the sample vessel. The pressure in the vessel was about 5×10^5 Pa, so the measured air volume was about 26 L in 1-atm pressure. Then the sample was measured using a NaI(Tl) spectrometer. The measured spectrum was compared with the preceding background spectrum, if the increased count rate was lower than the preset value, a conclusion of no contamination could be made. Then another sampling and measurement cycle was run. Otherwise, the cleaning process was run. The sample was removed by repeated pumping and flushing, and the residual spectrum was measured as the new background spectrum.

Methods used to reduce the memory effect were investigated. In the initial design, no grid was set in the sample vessel. Due to the large capacity of the sample vessel and the high pressure in it, noble gas was more easily adsorbed on its surface. The cleaning process of five pump-and-flush cycles could not remove the residual noble gas effectively. So grids were set in the sample vessel to increase the velocity of nitrogen airflow passing through the internal surface of the sample vessel, and this reduced the adsorption percentage by about one order of magnitude.

The method used to analyze the measured spectra was investigated. If background counts caused by low energy gamma-rays and Compton scatter radiation generated by high energy gamma-rays in the 81-keV ROI were too high, the stripping method was a useful tool to obtain the net count generated by ^{133}Xe in the sample.

Calibration coefficients and MDCs of ^{133}Xe, ^{135}Xe and ^{41}Ar were also calculated. The MDC level of the developed monitoring equipment was obviously lower than for other online monitoring equipment.

Author statement

Huibin Li: Project administration, Conceptualization, Methodology, Formal analysis, Investigation.
Weiguo Lei: Software, Validation.
Tiancheng Feng: Conceptualization, Supervision.
DingWei Huang: Software, Formal analysis.
Zining Tian: Formal analysis, Investigation.

Declaration of competing interest

None.

Acknowledgement

Appendix A. Supplementary data

Supplementary data to this article can be found online at https://doi.org/10.1016/j.apradiso.2020.109230.

References

Bläckberg, L., Fay, A., Jogi, I., 2011. Investigations of surface coatings to reduce memory effect in plastic scintillator detectors used for radioxenon detection. Nucl. Instrum. Methods Phys. Res. 656, 84–91.

Bläckberg, L., Fritioff, T., Martensson, L., 2013. Memory effect, resolution, and efficiency measurements of an Al_2O_3 coated plastic scintillator used for radioxenon detection. Nucl. Instrum. Methods Phys. Res. 714, 128–135.

Cooper, M.W., Mcintyre, J.I., Bowyer, T.W., 2007. Redesigned β-γ radioxenon detector. Nucl. Instrum. Methods Phys. Res. 579, 426–430.

Mirion Technologies Inc, 2002. NGM 204-L User Manual. MGPI.

Ringbom, A., Larson, T., Axelsson, A., Elmgren, K., Johansson, C., 2003. SAUNA-a system for automatic sampling, processing, and analysis of radioactive xenon. Nucl. Instrum. Methods Phys. Res. 508, 542–553.

Yongchun, X., Tieshuan, F., Chuanfei, Z., Fei, L., Qian, W., Rende, Z., Qingpei, X., 2017. Studies on adsorption-desorption of xenon on surface of BC-404 plastic scintillator based on soaking method. Nucl. Instrum. Methods Phys. Res. 847, 99–103.